PNAS RESEARCH ARTICLE | APPLIED BIOLOGICAL SCIENCES

Statins enhance the efficacy of HER2-targeting radioligand therapy in drug-resistant gastric cancers

Yi Rao[a], Zachary Samuels[a], Lukas M. Carter[a], Sebastien Monette[b], Sandeep Surendra Panikar[c], Patricia M. R. Pereira[c,1], and Jason S. Lewis[a,d,e,1]

Edited by Josep Tabernero, Vall d'Hebron Hospital, Barcelona, Spain; received November 30, 2022; accepted March 3, 2023 by Editorial Board Member Nancy Carrasco

Human epidermal growth factor receptor 2 (HER2) is overexpressed in various cancer types. HER2-targeting trastuzumab plus chemotherapy is used as first-line therapy for HER2-positive recurrent or primary metastatic gastric cancer, but intrinsic and acquired trastuzumab resistance inevitably develop over time. To overcome gastric cancer resistance to HER2-targeted therapies, we have conjugated trastuzumab with a beta-emitting therapeutic isotope, lutetium-177, to deliver radiation locally to gastric tumors with minimal toxicity. Because trastuzumab-based targeted radioligand therapy (RLT) requires only the extramembrane domain binding of membrane-bound HER2 receptors, HER2-targeting RLT can bypass any resistance mechanisms that occur downstream of HER2 binding. Leveraging our previous discoveries that statins, a class of cholesterol-lowering drugs, can enhance the cell surface-bound HER2 to achieve effective drug delivery in tumors, we proposed that the combination of statins and [^{177}Lu]Lu-trastuzumab-based RLT can enhance the therapeutic efficacy of HER2-targeted RLT in drug-resistant gastric cancers. We demonstrate that lovastatin elevates cell surface HER2 levels and increases the tumor-absorbed radiation dose of [^{177}Lu]Lu-DOTA-trastuzumab. Furthermore, lovastatin-modulated [^{177}Lu]Lu-DOTA-trastuzumab RLT durably inhibits tumor growth and prolongs overall survival in mice bearing NCI-N87 gastric tumors and HER2-positive patient-derived xenografts (PDXs) of known clinical resistance to trastuzumab therapy. Statins also exhibit a radioprotective effect, reducing radiotoxicity in a mice cohort given the combination of statins and [^{177}Lu]Lu-DOTA-trastuzumab. Since statins are commonly prescribed to patients, our results strongly support the feasibility of clinical studies that combine lovastatin with HER2-targeted RLT in HER2-postive patients and trastuzumab-resistant HER2-positive patients.

human epidermal growth factor receptor 2 (HER2) | radioligand therapy | trastuzumab | statins | trastuzumab-resistant cancer

Significance

Trastuzumab and trastuzumab-based drug resistance is a clinical challenge in recurrent and primary metastatic gastric cancers. Not all tumors respond to trastuzumab-based therapy and resistance is observed in the ones that show initial response. Because trastuzumab-based systemic endoradiotherapy requires only the extramembrane domain binding of membrane-bound Human epidermal growth factor receptor 2 (HER2) receptors, HER2-targeting radioimmunotherapy can bypass any resistance mechanisms that occur downstream of HER2 binding. We repurposed statins to enhance cell-surface HER2 availability in ways that increase tumor-to-nontarget–organ absorbed dose ratios and enhance efficacy in tumors resistant to conventional trastuzumab therapy. Ultimately, statins improve the efficacy of systemic radioimmunotherapy in drug-resistant HER2+ EG patients.

In 2020, more than 1,000,000 new cases of gastric cancer were diagnosed, with 770,000 deaths estimated worldwide (1). Human epidermal growth factor receptor 2 (HER2) overexpression occurs in 10 to 20% of esophagogastric (EG) cancers and is associated with poor overall patient survival (2, 3). The humanized recombinant monoclonal antibody trastuzumab binds to the extramembrane domain of HER2, inhibiting the growth of HER2-dependent tumors (4, 5). HER2-targeting trastuzumab, in combination with chemotherapy, is used as first-line therapy to treat HER2-positive (HER2+) EG cancer patients (6, 7). Despite the drug's initial efficacy, intrinsic and acquired resistance to trastuzumab can develop after multiple regimens of trastuzumab-based therapy, conferring resistance to HER2+ cancers (8–10). To overcome trastuzumab resistance in advanced HER2+ cancers, antibody–drug conjugates with covalently linked cytotoxic moieties such as trastuzumab emtansine (T-DM1) were developed. T-DM1, however, failed to improve overall survival compared to standard chemotherapy, taxane, in HER2+ EG cancers clinically due to T-DM1 resistance (11, 12). Recently, trastuzumab deruxtecan (DS8201), a Food and Drug Administration (FDA)-approved antibody–drug conjugate with a cleavable tetrapeptide-based linker and a cytotoxic topoisomerase I inhibitor, demonstrated the potential for improved efficacy in patients with HER2+ advanced EG cancers (13). Nevertheless, drug resistance remains a major challenge in such diseases. Consequently, there is an unmet clinical need for therapeutic strategies that can prevent or overcome HER2 resistance in patients with HER2+ EG cancers.

Similar to antibody–drug conjugates, trastuzumab-based radiopharmaceutical conjugates require effective HER2 surface binding and internalization in order to bypass intrinsic or acquired resistance mechanisms downstream of HER2 binding. Trastuzumab is a well-characterized antibody for targeting HER2+ tumors and has been explored as a vehicle to specifically deliver radionuclide cargo for cancer diagnostics and therapeutics using

Author contributions: Y.R., P.M.R.P., and J.S.L. designed research; Y.R., Z.S., S.M., and S.S.P. performed research; Y.R., L.M.C., S.M., P.M.R.P., and J.S.L. analyzed data; and Y.R., P.M.R.P., and J.S.L. wrote the paper.

The authors declare no competing interest.

This article is a PNAS Direct Submission. J.T. is a guest editor invited by the Editorial Board.

[1]To whom correspondence may be addressed. Email: ribeiropereirap@wustl.edu or lewisj2@mskcc.org.

This article contains supporting information online at https://www.pnas.org/lookup/suppl/doi:10.1073/pnas.2220413120/-/DCSupplemental.

Published March 27, 2023.

positron emission tomography and for targeted radioligand therapy (RLT) (14–19). In contrast to external beam irradiation, radiolabeled antibody conjugates allow the systematic delivery of target-specific radiation to tumor sites systematically while minimizing radiation exposure to healthy tissues.

Lutetium-177 is a commonly used β-emitting therapeutic isotope with a relatively low emission energy ($E_{\beta\text{-max}}$ 0.49 MeV) and emission range (maximum 1.6 mm). It can deliver sufficient radiation to induce DNA double-strand breaks while limiting damage to nearby healthy tissues (20, 21). Taking advantage of these properties, lutetium-177-based RLTs have succeeded clinically. [^{177}Lu]Lu-DOTATATE (Lutathera®), a lutetium-177 radiolabeled peptide targeting somatostatin receptors on neuroendocrine tumors, was approved by the FDA for the treatment of gastroenteropancreatic neuroendocrine cancers in adults (22–24). In addition, [^{177}Lu]Lu-PSMA-617 was recently approved as second-line therapy for the treatment of prostate-specific membrane antigen (PSMA)-positive metastatic castration-resistant prostate cancers (25). Furthermore, various preclinical studies have demonstrated the efficacy of [^{177}Lu]Lu-trastuzumab in treating HER2+ breast cancers, unlocking the potential for [^{177}Lu]Lu-trastuzumab-based RLTs for cancer treatments (19). When compared with anti-HER2 antibody-based therapies that require frequent infusions of the drug, [177Lu]Lu-trastuzumab could require only a single infusion visit.

One important factor dictating the efficacy of trastuzumab-based lutetium-177 RLT is the availability of cell surface-bound HER2 and the effective internalization of the radiotherapeutic payload. Although HER2 exists in both plasma membrane-bound and cytosolic forms, only cell-surface receptors are viable targets for HER2-based targeted RLT. Caveolin1 (CAV-1), which anchors on lipid rafts in plasma membranes, mediates endocytosis of cell surface HER2 (Fig. 1*A*) (26–28). We previously demonstrated that CAV-1 tumoral protein levels inversely correlate with tumor HER2 membrane levels (26, 29). Furthermore, we demonstrated that statin-mediated CAV-1 depletion elevated membrane-localized HER2 levels by decreasing cholesterol content in plasma membrane, proving to be a potential pharmacological approach to modulate HER2–antibody binding and internalization (Fig. 1*A*) (26, 30, 31). In addition, we previously observed various levels of increased internalization of pHrodo-labeled T-DM1 with lovastatin treatment in a panel of gastric cancer cells containing varying levels of HER2 expression (32). Herein, we propose the use of statins to pharmacologically enhance cell-surface–bound HER-2 availability so as to enhance [^{177}Lu]Lu-trastuzumab binding and internalization in EG tumors, consequently increasing tumor-to-nontarget-organ absorbed dose ratios. Ultimately, statins improve the efficacy of RLT in drug resistance in HER2+ EG patients.

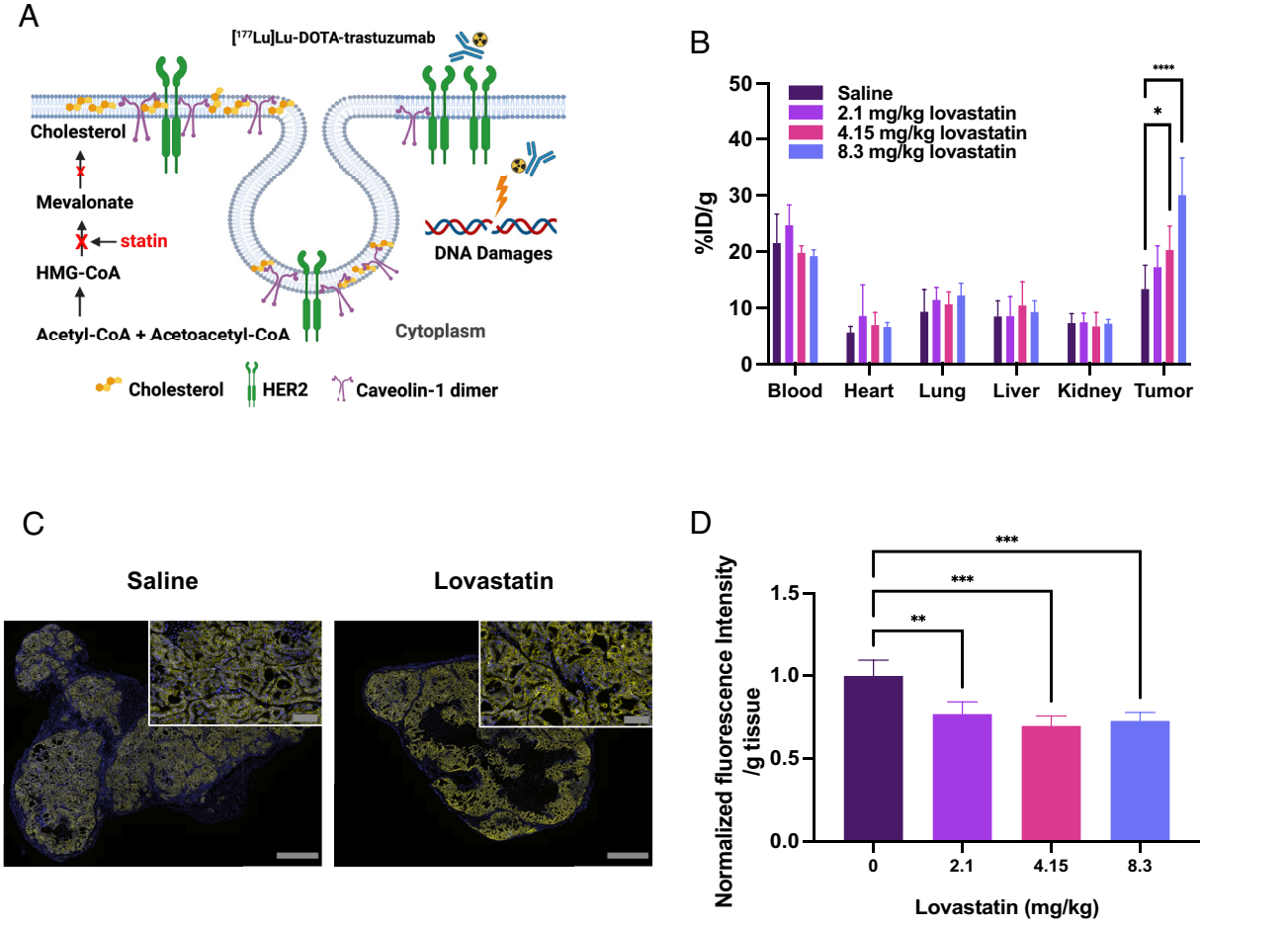

Fig. 1. Evaluating the role of lovastatin in modulating HER2 as mediated by CAV-1. (*A*) HER2 exists in either plasma-membrane–bound or cytosolic form. Only cell-surface receptors are available for trastuzumab therapy. Caveolin-1, which anchors on plasma membrane cholesterol, can internalize and degrade surface HER2. Previous studies showed that cholesterol-lowering drugs temporarily modulate plasma-membrane–bound CAV-1 levels, which further stabilizes cell-surface-associated HER2 in NCI-N87 cells. (*B*) Biodistribution data at 24-h post-injection of [^{89}Zr]Zr-DFO-trastuzumab in athymic nude mice bearing subcutaneous NCI-N87 tumors. Lovastatin was orally administrated. Tail vein injection of [^{89}Zr]Zr-DFO-trastuzumab (~5 μCi, 1.25 μg protein). Error bars, n = 4 mice per group, mean ± SD. (*C*) Representative immunofluorescent imaging of HER2 in mice tumors pretreated with saline and lovastatin. DAPI stained in blue and HER-2 in yellow. (Scale bars represent 100 μm for insets and 1 mm for the main images.) (*D*) Tumor cholesterol contents were extracted immediately after the second dose of lovastatin and evaluated using fluorometric assays. *P < 0.05, **P < 0.005, ***P < 0.0005, ****P < 0.00001.

Results

Statins Pharmacologically Modulate Membrane-Bound HER2 via Cholesterol-Mediated Mechanisms. Lovastatin, a cholesterol-depleting drug, reduces tumoral CAV-1 protein levels by lowering cholesterol in caveolae/lipid rafts, to which CAV-1 anchors in the cell (Fig. 1*A*). In previous studies, we demonstrated that lovastatin-induced CAV-1 depletion temporally enhances HER2 availability at the cell membrane, resulting in improved trastuzumab or trastuzumab-drug binding and efficacy (26) (Fig. 1*A*). Furthermore, among three chemically distinct statins, lovastatin demonstrated a greater ability to enhance antibody–tumor binding for cell surface receptors including PSMA and EGFR epidermal growth factor receptor than did two other chemically distinct statins, simvastatin and rosuvastatin (31). Here, we sought to determine the ability of lovastatin to enhance HER2-targeted radioimmunotherapy in tumors while reducing off-target doses to non-tumor tissues.

First, we determined the correlation between lovastatin doses, trastuzumab–tumor binding, and HER2 membrane levels in tumors from mice xenografted with the HER2+ EG tumors cell line NCI-N87. Lovastatin dose titration was conducted to determine levels of surface HER2, which was quantitatively measured as [^{89}Zr]Zr-DFO-trastuzumab accumulation in NCI-N87 tumors. Oral administration of saline or lovastatin at doses of 2.10, 4.15, and 8.30 mg/kg was performed 12 h prior to and simultaneously with the tail vein injection of [^{89}Zr]Zr-DFO-trastuzumab in *nu/nu* mice bearing NCI-N87 tumors. The lovastatin doses used in our animal studies correspond to human-equivalent doses of 0.17, 0.34, and 0.68 mg/kg, which are significantly lower than the maximum recommended daily dose of 1.33 mg/kg in humans (26, 33). We demonstrated that increasing doses of lovastatin from 0 to 8.3 mg/kg elevates [^{89}Zr]Zr-DFO-trastuzumab tumor uptake up to ~two-fold compared to saline-treated control groups with NCI-N87 xenografts (Fig. 1*B*). Enhanced surface HER2 levels were further confirmed with HER2 immunofluorescent imaging (Fig. 1*C*). An increase in cell surface tumoral HER2 was accompanied by a decrease in tumor cholesterol in mice administered lovastatin (Fig. 1*D*).

These data support the claims that lovastatin pharmacologically elevates cell surface HER2 levels, enhances trastuzumab–tumor binding, and reduces cholesterol contents in the plasma membrane of tumors.

Kinetics of Statin-Modulated [^{177}Lu]Lu-DOTA-Trastuzumab Biodistribution and Dosimetry Analyses for Potential Toxicity. Having observed that lovastatin enhances [^{89}Zr]Zr-DFO-trastuzumab tumor uptake, we then evaluated the kinetics and potential radiotoxicity of the theranostic pair [^{177}Lu]Lu-DOTA-trastuzumab RLT with and without oral administration of lovastatin. We performed [^{177}Lu]Lu-DOTA-trastuzumab biodistribution studies and transposed the organ time activity data into a computational mouse phantom to determine time-integrated activity coefficients and absorbed doses in mouse organs. Our previous studies demonstrated that two doses of oral 4.15 mg/kg lovastatin at 12-h intervals robustly enhanced membrane HER2 content (26). Hence, oral 4.15 mg/kg lovastatin or saline was administrated to *nu/nu* mice bearing NCI-N87 tumors both 12 h prior to and at the time of tail vein injection of [^{177}Lu]Lu-DOTA-trastuzumab. Increased [^{177}Lu]Lu-DOTA-trastuzumab tumor accumulations were observed over 144 h post-injection. At 72 h postinjection, a ~96% increase was observed in the lovastatin-treated group compared to saline-treated control group (Fig. 2 *A–E*). Using extrapolated time integrated activity coefficients, the theoretical absorbed dose coefficients with saline and lovastatin pretreatments were calculated (Fig. 2*F*). In addition, the theoretical absorbed doses of mouse organs were calculated for 250, 750, and 1,000 μCi [^{177}Lu]Lu-DOTA-trastuzumab injections. These values were compared to TD5/5 (5% risk of complication over 5 y) and TD50/5 (50% risk of complication over 5 y) to help identify potential dose-limiting organs (Fig. 2*G*) (34, 35). Consistent with previous lovastatin dose biodistribution studies, the dosimetry calculation indicated that statin improved the tumors' absorbed dose. The dosimetry calculation suggested the dose-limiting organ to be hematopoietic bone marrow, with possible lung toxicity at administered activities exceeding 750 μCi.

Together, these data demonstrate that lovastatin pretreatment enhanced tumor-absorbed radiation dose of [^{177}Lu]Lu-DOTA-trastuzumab.

Therapeutic Efficacy of Lovastatin-Modulated [^{177}Lu]Lu-DOTA-Trastuzumab Therapy in Mice Bearing HER2+ EG Xenografts. We assessed the therapeutic efficacy of the lovastatin-modulated [^{177}Lu]Lu-DOTA-trastuzumab approach via a dose-escalation study of 0, 250, 750, and 1,000 μCi (0, 9, 28, and 37 MBq; 50 μg) of [^{177}Lu]Lu-DOTA-trastuzumab with or without lovastatin pretreatment in mice bearing NCI-N87 tumors (Fig. 3*A*). Briefly, when tumor volumes reached ~400 to 500 mm^3, two doses of either lovastatin (4.15 mg/kg) or saline were orally administrated 12 h prior to and at the same time as the tail vein injection of [^{177}Lu]Lu-DOTA-trastuzumab. Isotope control cohorts of [^{177}Lu]Lu-IgG (250, 750, 1,000 μCi; 50 μg) were also included in the study. Typically, therapeutic regimens of weekly ~5 mg/kg trastuzumab are used for preclinical trastuzumab therapy, and NCI-N87 tumors relapse around 35 to 42 d after therapy (26). In contrast, a single dose of 50 μg (2 mg/kg) of unlabeled trastuzumab with or without statin pretreatment demonstrated a similar tumor growth rate and overall survival (Fig. 3 *B–F* and *SI Appendix*, Table S1). The modest tumor growth inhibitions and improved overall survival were observed in the cohorts given 250 μCi [^{177}Lu]Lu-DOTA-trastuzumab with and without statin pretreatment (Fig. 3 *C–G* and *SI Appendix*, Table S1). Importantly, the cohort given the combination of lovastatin and 750 μCi [^{177}Lu]Lu-DOTA-trastuzumab demonstrated durable tumor growth inhibition and prolonged overall survival up to 90 d (Fig. 3 *D–H* and *SI Appendix*, Table S1). By contrast, 2 wk after [^{177}Lu]Lu-DOTA-trastuzumab injections, mice in 750 μCi [^{177}Lu]Lu-DOTA-trastuzumab and [^{177}Lu]Lu-DOTA-IgG cohorts experienced severe petechiae and lethargy, indicators of severe radiotoxicity requiring euthanasia (Fig. 3 *H–J*). Furthermore, all 1,000 μCi [^{177}Lu]Lu-DOTA-trastuzumab cohorts showed signs of severe radiotoxicity regardless of the addition of lovastatin (Fig. 3 *E–I*), as predicted in the previous dosimetry calculations (Fig. 2*G*).

The reduced radiotoxicity in the cohort administered 750 μCi [^{177}Lu]Lu-DOTA-trastuzumab in combination with lovastatin supports the potential radioprotective effects of lovastatin, which has also been previously reported to inhibit ionizing-radiation-induced DNA damage-dependent stress responses and to promote DNA repair in normal tissues (36, 37). To further validate the radioprotective effect of lovastatin in NCI-N87 cells, we evaluated levels of γH2AX, an indicator of DNA damage, in response to various doses of targeted RLT. Treatment of NCI-N87 cancer cells with 25 μM lovastatin resulted in decreased γH2AX in cells treated with 10 to 1,000 μCi [^{177}Lu]Lu-DOTA-trastuzumab after 72 h, implying reduced accumulation of DNA damage and the radioprotective effect of lovastatin (*SI Appendix*, Fig. S1*A*).

In addition to physical signs of radiotoxicity due to RLT, weekly complete blood count analyses were performed to evaluate radiotoxicity. The counts of red blood cells, platelets, and white blood cells all dropped a week after the administration of radiopharmaceuticals and gradually recovered back to starting levels at week 4 (*SI Appendix*, Fig. S2).

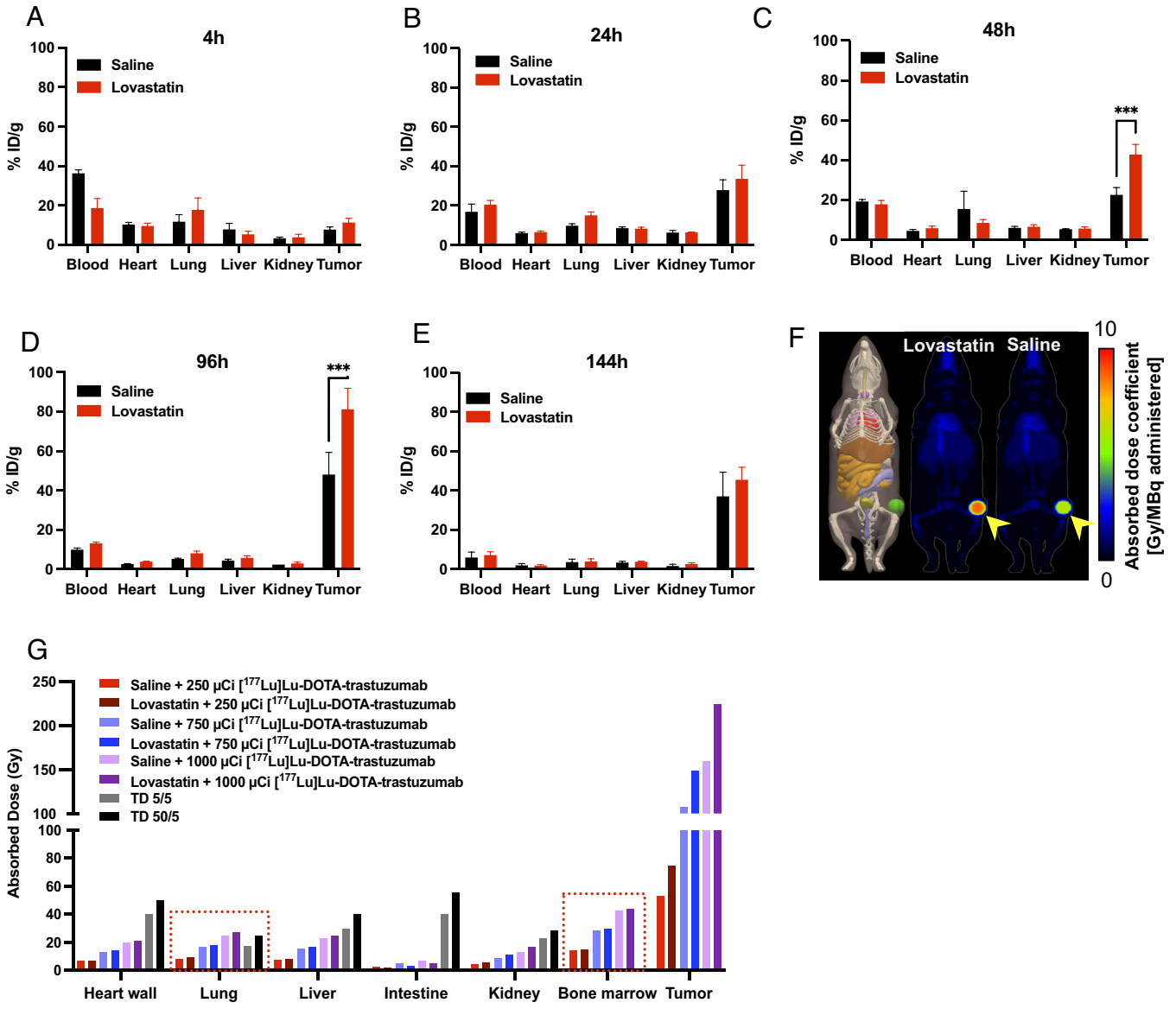

Fig. 2. Ex vivo biodistribution of [^{177}Lu]Lu-DOTA-trastuzumab in subcutaneous xenograft model of NCI-N87 with or without lovastatin pre-treatment. (*A–E*) Biodistribution data at 4 to 144 h post-injection of [^{177}Lu]Lu-DOTA-trastuzumab in mice bearing NCIN87 tumors. Tail vein injection of [^{177}Lu]Lu-DOTA-trastuzumab (~5 µCi, 1.25 µg protein). Error bars, n = 4 mice per group, mean ± SD. (*F*) Dosimetry calculation of tumor absorbed doses when treated with lovastatin and saline. (*G*) Dosimetry calculation of absorbed dose for different organs at different doses of lutetium-177. ***$P < 0.0005$.

Taken together, these results strongly suggest that statin-modulated [^{177}Lu]Lu-DOTA-trastuzumab RLT durably inhibits tumor growth and prolongs overall survival. Additionally, lovastatin exhibited a radioprotective effect by systematically mitigating radiotoxicity and improving overall survival.

Statin-Modulated HER2 RLT Demonstrated Durable Responses Against Drug Resistance in Esophagogastric Cancers. To further evaluate the impact of HER2 RLT combined with lovastatin in HER2+ trastuzumab-resistant EG tumors, HER2- and CAV-1-positive EG patient-derived xenografts (PDXs) with known, clinically developed HER2 resistance were implanted into athymic nude mice. Biodistribution studies of [^{177}Lu]Lu-DOTA-trastuzumab with and without lovastatin were performed and tumor uptake of [^{177}Lu]Lu-DOTA-trastuzumab was found to have increased by ~48% in the cohort pretreated with lovastatin compared to the saline control (Fig. 4*A*). This suggested that lovastatin treatment improved the tumor-absorbed doses of [^{177}Lu]Lu-DOTA-trastuzumab, which indicates a more efficacious RLT.

To assess the efficacy of [^{177}Lu]Lu-DOTA-trastuzumab therapy combined with lovastatin, we performed RLT in mice bearing HER2-positive gastric PDXs. Because the biodistributions of radiopharmaceutical tumor uptake in both NCI-N87 and PDX models were comparable, 750 µCi (28 MBq) [^{177}Lu]Lu-DOTA-trastuzumab was used in the PDX RLT. When tumor volumes reached ~500 to 600 mm^3, two doses of lovastatin (4.15 mg/kg) or saline were orally administrated both 12 h prior to and at the time of intravenous injection of 750 µCi [^{177}Lu]Lu-DOTA-trastuzumab (50 µg) or [^{177}Lu]Lu-DOTA-IgG (50 µg). Mice treated with either a single dose of trastuzumab (median survival = 17 d) or trastuzumab combined with lovastatin (median survival = 19.5 d) showed the fastest tumor growth and poorest overall survival compared to [^{177}Lu]Lu-DOTA-trastuzumab-treated cohorts (Fig. 4 *B–D*). Furthermore, less than 3 wk after RLT, more than 50% of the mice from the [^{177}Lu]Lu-DOTA-IgG isotype control cohort experienced severe petechiae and lethargy, requiring euthanasia. It is important to note that tumor growth inhibitions were observed in both [^{177}Lu]Lu-DOTA-trastuzumab-treated cohorts, but the

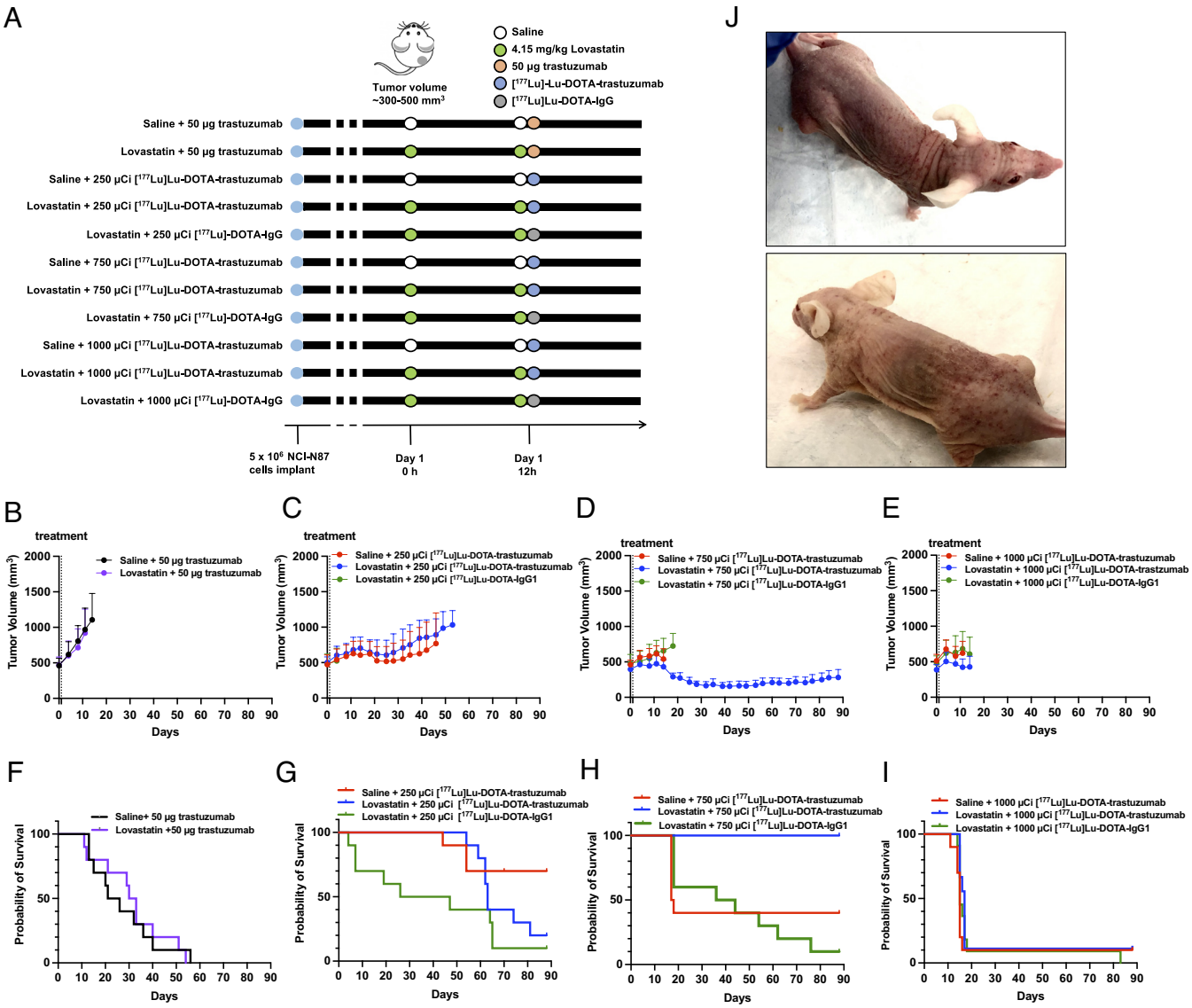

Fig. 3. [^{177}Lu]Lu-DOTA-trastuzumab dose escalation endoradiotherapy with or without lovastatin pre-treatments in NCI-N87 bearing mice. (*A*) Targeted RLT scheme illustrating all therapeutic treatment groups and timelines. Tail vein injection of [^{177}Lu]Lu-DOTA-trastuzumab (~0 to 1,000 µCi, 50 µg protein total). (*B* and *D–F*) mean tumor growth for each treatment group; Error bars, n = 10 mice per group, mean ± SD. Mean tumor growth was calculated until the termination of the first mouse in the given group. (*C* and *G–I*) Median survival of mice bearing NCI-N87 tumors post-treatment. Log-rank tests were performed to compare each treatment with saline cohort. ****$P < 0.0001$. (*J*) Representative images of mice experiencing severe petechiae.

cohort undergoing combination treatment of [^{177}Lu]Lu-DOTA-trastuzumab and lovastatin demonstrated durable tumor growth inhibition and remarkably prolonged survival compared to all other cohorts (Fig. 4 *B–D*). By contrast, tumors of the [^{177}Lu]Lu-DOTA-trastuzumab monotherapy cohort exhibited initial growth suppression, but eventually relapsed 40 d post-treatment (Fig. 4*B*), suggesting that [^{177}Lu]Lu-DOTA-trastuzumab combined with statin pretreatment exerted durable tumor growth inhibition in HER2+ trastuzumab-resistant EG PDXs.

Similar to the previous dose escalation study using the NCI-N87 xenograft model, weekly complete blood count analyses were performed in the PDX model to evaluate radiotoxicity. The counts of red blood cells, platelets, and white blood cells dropped during the week following the administration of the radiopharmaceuticals. Levels of red blood cells, platelets, and white blood cells recovered to their normal ranges (the mean ± 2 SD of values collected from the entire cohort) 1 wk later in [^{177}Lu]Lu-DOTA-trastuzumab-treated cohorts (with or without lovastatin), whereas [^{177}Lu]Lu-DOTA-IgG isotype control cohort groups demonstrated slower recovery due to severe radiotoxicity, manifested as severe petechiae and lethargy (*SI Appendix*, Fig. S3). Mice with severe petechiae and lethargy were sacrificed per IACUC guidelines.

Overall, these data demonstrate further the ability of lovastatin-modulated [^{177}Lu]Lu-DOTA-trastuzumab treatment to enhance therapeutic efficacy and prolong overall survival in trastuzumab-resistant HER2+ EG PDXs.

Discussion

While HER2-targeting trastuzumab is currently used as first-line therapy to treat HER2+ EG cancer patients (38, 39), intrinsic and acquired resistance to trastuzumab can develop over time (39). Antibody–radiopharmaceutical conjugates, however, can potentially overcome drug resistance associated with downstream HER2 signaling. In addition, lutetium-177-radiolabeled trastuzumab provides systemic and target-specific delivery of β-emission therapy, which leads to accumulated DNA damage at tumor sites. Collectively, we utilize lovastatin to pharmacologically elevate

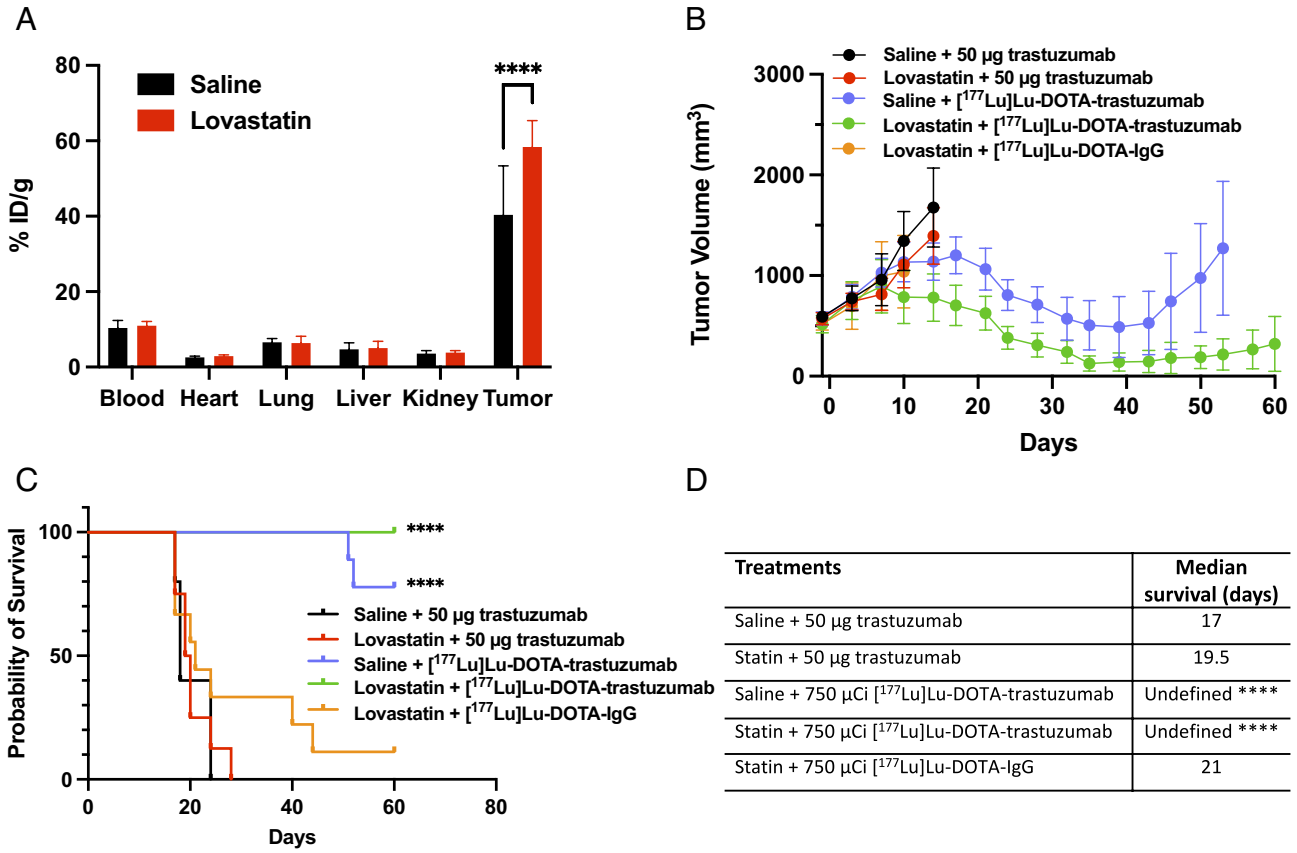

Treatments	Median survival (days)
Saline + 50 µg trastuzumab	17
Statin + 50 µg trastuzumab	19.5
Saline + 750 µCi [^{177}Lu]Lu-DOTA-trastuzumab	Undefined ****
Statin + 750 µCi [^{177}Lu]Lu-DOTA-trastuzumab	Undefined ****
Statin + 750 µCi [^{177}Lu]Lu-DOTA-IgG	21

Fig. 4. Endoradiotherapy with HER-2 modulation in PDXs. (*A*) Biodistribution data at 48-h post-injection of [^{177}Lu]Lu-DOTA-trastuzumab in athymic nude mice bearing PDXs. Tail vein injection of [^{177}Lu]Lu-DOTA-trastuzumab (~5 µCi, 1.25 µg protein). Error bars, n = 4 mice per group, mean ± SD. (*B* and *C*) Enhanced therapeutic efficacy in tumor growth and overall survival at 750 µCi [^{177}Lu]Lu-DOTA-trastuzumab (50 µg protein) with or without statin pre-treatment in mice bearing HER2+ PDXs, as compared to saline and IgG control groups. (*D*) Median survival of mice bearing PDXs post-treatment. Log-rank tests were performed to compare each treatment with saline cohort. Error bars, n = 9 to 10 mice per group, mean ± SD. ****$P < 0.0001$.

membrane-bound HER2 availability and [^{177}Lu]Lu-DOTA-trastuzumab payload internalization, resulting in improved therapeutic efficacy compared to trastuzumab or trastuzumab–drug conjugates (26, 32). Hence, the combination of statin and [^{177}Lu]Lu-DOTA-trastuzumab in HER2+ EG tumor models was evaluated as a proof-of-concept for the combination strategy.

Multi-timepoint biodistribution studies of [^{177}Lu]Lu-DOTA-trastuzumab with or without statins using the NCI-N87 model showed that lovastatin enhanced [^{177}Lu]Lu-DOTA-trastuzumab tumor uptake and consequently increased tumor-absorbed radiation. However, it was also found that the 250 µCi [^{177}Lu]Lu-DOTA-trastuzumab cohort demonstrated similarly effective tumor growth inhibition over time compared to the statin-modulated 250 µCi [^{177}Lu]Lu-DOTA-trastuzumab cohort (Fig. 3 *C*–*G*). We attributed this finding to longstanding observations in the radiotherapy literature documenting that statins, inhibitors of 3-hydroxy-3-methyl-glutaryl-coenzyme A reductase, have pleiotropic effects contributing to radioprotection (36, 40). Statins reduce radiation-induced DNA double-strand breaks by accelerating DNA repairs and exhibit anti-inflammatory effects after radiation treatments by inhibiting inflammatory kinases, including Rho and Rho-associated protein kinases (41). Collectively, various statins, including lovastatin and simvastatin, reduce radiation-induced toxicities in normal tissues (42). Lovastatin (20 µM) has been reported to dampen ionizing radiation without DNA double-strand breaks in human umbilical vein endothelial cells (36). Furthermore, weekly treatments of lovastatin (10 mg/kg) in mice demonstrated reduced ionizing-radiation-induced DNA damage in lung tissue (37). Herein, the pretreatment of lovastatin could attenuate the efficacy of radiopharmaceuticals as observed in the 250 µCi [^{177}Lu]Lu-DOTA-trastuzumab-treated cohorts. To confirm the radioprotective effect of lovastatin, we evaluated the accumulated DNA damage in NCI-N87 cells incubated with various doses of [^{177}Lu]Lu-DOTA-trastuzumab with or without lovastatin. Lovastatin treatment dampened the γH2AX signal, an indicator of DNA damage, implying that lovastatin indeed exhibits a radioprotective effect against Lu-177-mediated β-therapy (*SI Appendix*, Fig. S1*A*). This implication is consistent with previous studies demonstrating that Rho inhibition via lovastatin enhanced the repair of radiation-induced DNA double-strand breaks (36, 37).

In the dose escalation studies of [^{177}Lu]Lu-DOTA-trastuzumab in mice bearing HER2+ NCI-N87 tumors, the combination of statin and 750 µCi [^{177}Lu]Lu-DOTA-trastuzumab demonstrated the most substantial and durable tumor growth inhibition as well as prolonged survival, while 750 µCi [^{177}Lu]Lu-DOTA-trastuzumab alone resulted in severe radiotoxicity and decreased overall survival (Fig. 3). The cohort combining lovastatin and 750 µCi [^{177}Lu]Lu-DOTA-trastuzumab successfully recovered from all physical signs of radiotoxicity due to the radioprotective effect of lovastatin for normal organs, while tumor sites saw continued therapeutic efficacy, highlighting the known radioprotective effect of lovastatin on normal tissues. At a lower administered activity (250 µCi [^{177}Lu]Lu-DOTA-trastuzumab), statin pretreatment attenuated the efficacy of β-therapy by reducing radiation-induced DNA damages manifested as moderate γH2AX signals (*SI Appendix*, Fig. S1*B*). However, the observed statin-mediated radioprotective effects could eventually be overcome at the higher dose of 750 µCi

[^{177}Lu]Lu-DOTA-trastuzumab. Comparable levels of γH2AX signals were observed with and without lovastatin pretreatment, effectively inhibiting tumor growth, prolonging survival, and reducing radiotoxicity (*SI Appendix*, Fig. S1*B*). In our own studies, with an optimized balance of statin and radiopharmaceuticals, statin pretreatment increased tumor uptake of radiopharmaceuticals and durably inhibited tumor growth while minimizing radiation-induced radiotoxicity by providing radioprotection to normal tissue.

In the light of recent success and clinical approval of HER2-targeting ADCs, trastuzumab-deruxtecan demonstrated advanced efficacy on gastric tumors in the clinic. Hence, we compared the efficacies of T-DXd with lovastatin + 750 μCi [^{177}Lu]Lu-DOTA-trastuzumab in NCI-N87 tumor-bearing mice (*SI Appendix*, Fig. S4*A*). Mice treated with 10 mg/kg T-DXd demonstrated tumor response inhibition, but weight loss and necrosis were also observed (*SI Appendix*, Fig. S4*B*). Treatment with 5 mg/kg T-DXd significantly inhibited tumor growth on a level comparable to the lovastatin + 750 μCi [^{177}Lu]Lu-DOTA-trastuzumab-treated cohort (*SI Appendix*, Fig. S4*A*). These results suggested comparable efficacies for lovastatin + 750 μCi [^{177}Lu]Lu-DOTA-trastuzumab and 5 mg/kg T-DXd in NCI-N87 tumors.

In the context of trastuzumab-resistant HER2+ EG PDXs, 750 μCi [^{177}Lu]Lu-DOTA-trastuzumab with or without statin demonstrated significant tumor growth inhibition and prolonged survival compared to trastuzumab control groups or 750 μCi [^{177}Lu]Lu-DOTA-IgG control groups (Fig. 4 *B*–*D*). It is noteworthy that, although we observed an initial tumor growth inhibition 2 wk post-RLT in the cohort treated with 750 μCi [^{177}Lu]Lu-DOTA-trastuzumab monotherapy, a relapse occurred around week 6. Our previous studies in that same EG PDX model demonstrated resistance to trastuzumab or the trastuzumab–drug conjugate T-DM1 (26, 32). In contrast, the statin-modulated 750 μCi [^{177}Lu]Lu-DOTA-trastuzumab combination therapy cohort again demonstrated durable growth inhibition and prolonged survival (Fig. 4 *B* and *C*). Collectively, these results demonstrated that HER2-targeting RLT combined with lovastatin-delayed trastuzumab resistance in HER2+ EG PDXs. In addition, both therapeutic studies demonstrated that a single dose of [^{177}Lu]Lu-DOTA-trastuzumab (750 μCi, 50 μg) in combination with lovastatin was sufficient for durable growth inhibition and prolonged survival in mice bearing HER2+ EG cancers. Conventional trastuzumab therapies normally require higher doses of trastuzumab with multiple treatment regimens, whereas statin-modulated [^{177}Lu]Lu-DOTA-trastuzumab radiotherapy could potentially prevent or delay drug resistance in HER2+ EG cancers.

All mice receiving RLT experienced transient radiotoxicity, which manifests as decreased counts of red blood cells, white blood cells, and platelets 1 wk after the administration of radiopharmaceuticals. However, red blood cell, white blood cell, and platelet counts recovered back to their corresponding normal ranges over time (*SI Appendix*, Figs. S2 and S3). Severe radiotoxicity was observed in all 1,000 μCi [^{177}Lu]Lu-DOTA-trastuzumab or [^{177}Lu]Lu-DOTA-IgG groups as predicted based on the previous dosimetry calculation (Fig. 2*G*). Higher doses of radiopharmaceuticals resulted in both enhanced tumor-absorbed dose and an increased risk of systematic radiotoxicity, suggesting a fine balance between the efficacy of RLT and radiotoxicity. However, the pretreatment of lovastatin-protected mice bearing NCI-N87 tumors from the severe radiotoxicity otherwise caused by 750 μCi [^{177}Lu]Lu-DOTA-trastuzumab treatment as compared to saline pretreated and IgG isotype control cohorts (Fig. 3). Furthermore, in the mice implanted with trastuzumab-resistant PDXs, severe radiotoxicity was only observed in mice treated with 750 μCi [^{177}Lu]Lu-DOTA-IgG. These data again indicated that the dual effect of lovastatin enhances tumor uptake of radiopharmaceuticals, improves therapeutic efficacy via increased target availability, and systematically protects mice from radiotoxicity through its radioprotective effects.

Despite the enhanced therapeutic efficacy of statin-modulated [^{177}Lu]Lu-DOTA-trastuzumab RLT, it is acknowledged that, in addition to HER2 modulation, statins could potentially exhibit other off-target effects that were not fully interrogated in our study, although statins are commonly used and well-tolerated clinically. Furthermore, the human tumor xenografts used in this study only accounted for trastuzumab–tumor binding, since trastuzumab does not react with murine HER2. Hence, any potential enhanced HER2 expression in non-tumor tissues (murine tissues) was not accounted for. Also, since *nu/nu* mice are immunocompromised, our study fails to capture the interaction between RLT and immune responses.

Although we extensively evaluated the efficacy of statin-modulated [^{177}Lu]Lu-DOTA-trastuzumab radiotherapy in HER2+ EG tumors, potential applications of this combination strategy are not limited to EG cancers or to HER2+ tumors. We previously reported that in BT474, a HER2+ breast cancer cell line, the combination of statins and trastuzumab inhibited tumor growth over treatment with either trastuzumab or lovastatin alone (26). These data strongly supported the potential translation of combined statins and RLT to HER2+ breast cancers as well. In addition to their various applications in HER2+ cancer models, the data show that statins can also modulate the membrane availability of other receptors, including EGFR (epidermal growth factor receptor) and PSMA (31). The evidence that statins pharmacologically enrich membrane-bound EGFR and PSMA suggests they can be combined with other therapies targeting these receptors. With the recent FDA approval of [^{177}Lu]Lu-PSMA-617 for treating PSMA+ metastatic castration-resistant prostate cancers, statins could be combined with [^{177}Lu]Lu-PSMA-617 to enhance PSMA expression and therapeutic efficacy. In addition, because statins are known to attenuate the efficacy of α therapy via reduced radiation-induced DNA damage, we are investigating the combination of statins and trastuzumab-based α therapy (e.g., ^{225}Ac) with a higher emission energy and shorter effective range that could potentially overcome statin-induced radioprotection at the tumor site while protecting nearby normal tissues.

Collectively, our studies demonstrate that the combination of lovastatin and HER2-targeted RLT enhances therapeutic efficacy in HER2+ EG tumors as well as trastuzumab-resistant PDXs while also providing a systematic protective effect that mitigates radiotoxicity. Since statins are commonly prescribed to cancer patients, our results strongly support the feasibility of clinical studies combining lovastatin with HER2-targeted RLT in HER2+ patients and trastuzumab-resistant HER2+ patients.

Materials and Methods

Cell Line. Gastric cancer cell line NCI-N87 was obtained from the American Type Culture Collection (Manassas, VA). Cells were negative for mycoplasma contamination, and early passages (<10) were used in all studies. NCI-N87 cells were grown in RPMI-1640 growth medium supplemented with 10% fetal calf serum, 2 mM L-glutamine, 10 mM N-2-hydroxyethylpiperazine-N'-2-ethanesulfonic acid, 1 mM sodium pyruvate, 4.5 g/L glucose, 100 units/mL penicillin and streptomycin, and 1.5 g/L sodium bicarbonate. Cell cultures were maintained at 37 °C in a humidified 5% CO_2 atmosphere.

Conjugation and Radiolabeling of Trastuzumab.

Synthesis of [^{89}Zr]Zr-DFO-trastuzumab. Trastuzumab was conjugated with six-fold molar excess of desferrioxamine (DFO) (Macrocyclics, Inc.) chelator at a pH of 9 and 37 °C for 90 min on a thermomixer at 350 rpm. Trastuzumab-DFO conjugate was then purified by size exclusion chromatography on a PD-10 desalting

column (GE Healthcare) and concentrated with a 50 kDa Amicon centrifugal filter. The final concentration of the trastuzumab-DFO conjugate was quantitated by nanodrop (Thermo Fisher Scientific). Trastuzumab-DFO was diluted in 100 μL of saline at adjusted pH 7.0 and incubated with no-carrier-added [^{87}Zr]Zr-oxalate (3D Imaging limited liability company) at a ratio of 4:1 ([^{89}Zr]Zr-oxalate: antibody; μCi:μg). The immunoconjugates and [^{89}Zr]Zr-oxalate mixture was incubated for 1 h at 37 °C. The radioimmunoconjugate mixture was then purified using a PD-10 desalting column followed by 50 kDa Amicon Ultra centrifugal concentration. Purity was assessed using instant thin-layer chromatography (iTLC) with 50 mM ethylenediaminetetraacetic acid (EDTA) mobile phase. The purity of the purified radiolabeled antibody was >99%.

Synthesis of [^{177}Lu]Lu-DOTA-trastuzumab. Trastuzumab (Genentech) or isotope control antibody (IgG1) (MP Biomedicals) was conjugated with 20-fold molar excess of *p*-SCN-Bn-DOTA (Macrocyclics, Inc.) chelator at a pH of 9 and 37 °C for 90 min on a thermomixer at 350 rpm. The DOTA-modified immunoconjugates were purified by size exclusion chromatography on a PD-10 desalting column (GE Healthcare) and concentrated with a 50 kDa Amicon centrifugal filter. The DOTA-modified immunoconjugate was diluted in 100 μL of 250 mM NH_4OAc buffer at adjusted pH 5.5 and incubated with no-carrier-added [^{177}Lu]$LuCl_3$ (ITM, Germany) at a ratio of 20:1 for therapeutic applications or 4:1 for biodistribution studies ([^{177}Lu]$LuCl_3$:antibody; μCi:μg). The immunoconjugate and [^{177}Lu]$LuCl_3$ mixture was incubated for 1 h at 37 °C. The [^{177}Lu]Lu-DOTA-mAb was then purified using a PD-10 desalting column and concentrated by a 50 kDa Amicon Ultra centrifugal filter. Radiochemical purity was quantified by iTLC using 50 mM ethylenediaminetetraacetic acid (EDTA) as the eluent. The purity of the purified radiolabeled antibody was >99%.

NCI-N87 and patient-derived tumors xenograft (PDX) models. Animal experiments were performed in compliance with protocols approved by the Research Animal Resource Center and Institutional Animal Care and Use Committee at Memorial Sloan Kettering Cancer Center. A mixture of medium and Matrigel (BD Bioscience) (1:1 ratio) containing 5×10^6 NCI-N87 cells were injected subcutaneously into the right hind legs of 8-to-10-wk–old female athymic *nu/nu* mice (Crl:NU(NCr)-*Foxn1*^{nu} (Charles River Laboratories). PDX models were established by Memorial Sloan Kettering Cancer Center's Anti-tumor Assessment Core as reported previously (26). Briefly, patient-derived tumor specimens were collected following the protocols approved by the Research Animal Resource Center and Institutional Animal Care and Use Committee at Memorial Sloan Kettering Cancer Center. The PDX used in this study was derived from a patient who developed trastuzumab resistance clinically, and tumor tissue was confirmed to be HER2 and CAV-1+. Tumors were minced, and tumor/Matrigel mixtures were implanted subcutaneously in 7-to-9-wk–old female *nu/nu* athymic mice (Charles River Laboratory). Once established, tumors were maintained and expanded by series of subcutaneous transplantations.

Tumor volume was estimated by external vernier caliper measurements of the longest axis, *a*, and the axis perpendicular to the longest axis, *b*. The tumors were assumed to be spheroidal, and the volume was calculated using the equation $V = (4\pi/3) \times (a/2)^2 \times (b/2)$. The maximum allowed total tumor burden of 1,500 cm^3 for NCI-N87 model, and 2,000 cm^3 for the PDX model was not exceed in our experiments. n = 9 to 10 mice were used for each therapeutic cohort.

Biodistribution studies.

Lovastatin dose titration biodistribution studies. When tumor volumes reached ∼100 to 200 mm^3, mice were randomized into eight groups (n = 4 mice per group). Lovastatin at 0, 2.1, 4.15, or 8.3 mg/kg per mouse was orally administered 12 h before and at the same time as the tail vein injection of [^{89}Zr]Zr-DFO-trastuzumab (6 to 10 μCi, 2 μg). At 24 and 48 h, mice were sacrificed and organs were harvested, weighed, and measured in a gamma counter (PerkinElmer Wizard^2 2480). Radioactivity associated with each organ was expressed as percentage of injected dose normalized by grams of organ (% ID/g).

[^{177}Lu]Lu-DOTA-trastuzumab biodistribution studies. When tumor volumes reached ∼300 to 400 mm^3, mice were randomized into 10 groups (n = 5 mice per group). Saline or lovastatin at 4.15 mg/kg per mouse was orally administered 12 h before and at the same time as the tail vein injection of [^{177}Lu]Lu-DOTA-trastuzumab (6 to 10 μCi, 2 μg). At 4, 24, 48, 96, and 144 h, mice were killed and organs were harvested, weighed, and measured in a gamma counter. Radioactivity associated with each organ was expressed as the percentage of injected dose normalized by grams of organ (% ID/g).

Dosimetry. Murine organ time-integrated activity coefficients (TIACs (43) units of h or MBq · h /MBq) for [^{177}Lu]Lu-DOTA-trastuzumab, were estimated from the ex vivo biodistribution data (separately for saline and lovastatin cohorts). Uptake in the blood was assumed to be representative of uptake in the hematopoietic bone marrow. The %ID/g organ uptake values were converted to standardized uptake values (SUVs; normalized by total body mass) for extrapolation to a representative mouse computational phantom. The percentage of injected dose in phantom organ *I*, $\%ID_I$, was obtained from Eq. **1**, which assumes SUV is independent of body mass:

$$\%ID_I = SUV_i \cdot \frac{m_I}{m_{TB}} \times 100\,\%, \qquad [\mathbf{1}]$$

where SUV_i is the measured standardized uptake value for mouse organ *i*, m_I is the mass of corresponding phantom organ *I*, and m_{TB} is the total phantom mass. The $\%ID_I$ at each time point was subsequently multiplied by a corresponding radioactive decay factor. To obtain the TIACs, the resultant activity–time curves were integrated by the trapezoidal method over an interval spanning the time of injection to the last measured timepoint (144 h); beyond the last measured timepoint, clearance was assumed to occur via radioactive decay only and the analytical expression for the integral was used.

Using the derived TIACs, tumor and normal organ absorbed dose coefficients for the 25 g reference mouse (MOBY phantom) were computed using PARaDIM 1.0/Particle and Heavy Ion Transport Code System version 3.2 (44, 45). All PARaDIM parameter defaults for electron and photon transport were used; 2×10^7 total events were simulated, resulting in <2% statistical uncertainty in the organ-level dose coefficients.

Cholesterol quantification. Cholesterols were extracted from NCI-N87 tumor tissues from mice treated with or without lovastatin using the cholesterol extraction kit and following the manufacturers' instructions (Sigma-Aldrich). The extracted cholesterols were then dried at 50 °C to remove the trace amounts of organic solvent. Dried cholesterols were then reconstituted and quantified using the total cholesterol assay kit (Cell Biolabs, Inc.). The oxidation of the cholesterol was coupled with the reduction of hydrogen peroxide, which was then detected by a specific fluorescence probe emitting at 595 nm. Emission at 595 nm was measured using a SpectraMax i3 Multi-Mode Platform (Molecular Devices).

In vivo [^{177}Lu]Lu- DOTA-trastuzumab therapies. When tumor volumes reached ∼300 to 600 mm^3, mice were randomized into 11 groups, including saline + 50 μg trastuzumab, lovastatin + 50 μg trastuzumab, saline + 250 μCi [^{177}Lu]Lu-DOTA-trastuzumab, lovastatin + 250 μCi [^{177}Lu]Lu-DOTA-trastuzumab, lovastatin + 250 μCi [^{177}Lu]Lu-DOTA-IgG, saline + 750 μCi [^{177}Lu]Lu-DOTA-trastuzumab, lovastatin + 750 μCi [^{177}Lu]Lu-DOTA-trastuzumab, lovastatin + 750 μCi [^{177}Lu]Lu-DOTA-IgG, saline + 1,000 μCi [^{177}Lu]Lu-DOTA-trastuzumab, lovastatin + 1,000 μCi [^{177}Lu]Lu-DOTA-trastuzumab, and lovastatin + 1,000 μCi [^{177}Lu]Lu-DOTA-IgG. Lovastatin (4.15 mg/kg per mouse) or saline was orally administered 12 h before and at the same time as the tail vein injection of 250 to 1,000 μCi of [^{177}Lu]Lu-DOTA-trastuzumab or [^{177}Lu]Lu-DOTA-IgG (50 μg). Tumor volumes were measured twice a week for 90 d or until mice reached any of the following endpoints: severe petechiae, >20% weight loss, >1,500 mm^3 tumor volume for NCI-N87 xenografts, or >2,000 mm^3 tumor volume for the PDXs.

Immunofluorescence microscopy. Harvested subcutaneous NCI-N87 tumors were subjected to formalin-fix and paraffin-embedded sections (10 μm). Sections were then submitted to the Memorial Sloan Kettering Cancer Center Molecular Cytology Core for HER2 and γH2AX staining. Images of stained slides were acquired with a BX61 microscope, DP80 camera and cellSens Dimension 3.2 software (Olympus, Tokyo, Japan) and analyzed by a board-certified veterinary pathologist from the Memorial Sloan Kettering Cancer Center Comparative Pathology Core.

DNA damage assay. NCI-N87 cells were seeded on 96-well black wall clear bottom microplates at 100,000 cells per well 24 h before each experiment in its culture medium. On the day of the experiment, cells were pretreated with or without 25 μM of lovastatin (Sigma-Aldrich) 12 h prior to mirroring the statin treatment schedule in vivo. Then, 200 μL of medium containing 0 to 1,000 μCi of [^{177}Lu]Lu-DOTA-trastuzumab with or without lovastatin was added to each well. After 48 h of incubation, accumulated DNA damage was accessed by evaluating

the fluorophore of antibody-based γH2AX signals using the HCS DNA damage kit (Thermo Fisher Scientific), and total cell counts per well was evaluated using Hoechst 33342 (Thermo Fisher Scientific). The antibody-based γH2AX signals at 555 nm and Hoechst 33342 at 460 nm were measured using a SpectraMax i3 Multi-Mode Platform (Molecular Devices). Experiments were performed in triplicate, n = 3 independent experiments.

Radiotoxicity studies. Mice were monitored for physical signs of toxicity, including weight loss, lethargy, and petechiae. Briefly, mice were weighed twice a week, and retro-orbital blood was collected weekly for hematologic analyses. White blood cells, red blood cells, and platelets were evaluated using an Element HT5 (Heska Corporation) prior to the administration of radiotherapy and throughout the study. Mice with severe petechiae and lethargy were euthanized per Institutional Aminal Care and Use Committe (IACUC) guidelines.

T-DXd treatments. Animal experiments involving the use of T-DXd were performed following the guidelines approved by the Research Animal Resource Center and Institutional Animal Care and Use Committee at Washington School of Medicine at St. Louis. Mice bearing NCI-N87 tumors were intravenously injected with T-DXd (5 mg/kg or 10 mg/kg) and tumor volumes were determined by vernier caliper measurement twice a week.

Statistical analyses. All data are shown as mean values ± SD. Statistical analyses were performed using GraphPad Prism version 9.1. 2. A P value <0.05 was considered significant.

Data, Materials, and Software Availability. All study data are included in the article and/or *SI Appendix*.

ACKNOWLEDGMENTS. This study was supported in part by the Geoffrey Beene Cancer Research Center of Memorial Sloan Kettering Cancer Center, NIH R35 CA232130, NIH R01 CA244233-01A1. We gratefully acknowledge Mr. William H. and Mrs. Alice Goodwin and the Commonwealth Foundation for Cancer Research and The Center for Experimental Therapeutics of Memorial Sloan Kettering Cancer Center. American Cancer Society (IRG-21-133-64-03) for P.M.R.P. NIH (1R37CA276498-01) for P.M.R.P. We gratefully acknowledge the Siteman Cancer Center pharmacy for providing us with T-DXd/Enhertu antibodies.

Author affiliations: [a]Department of Radiology, Memorial Sloan Kettering Cancer Center, New York, NY 10065; [b]Laboratory of Comparative Pathology, Memorial Sloan Kettering Cancer Center, The Rockefeller University, Weill Cornell Medicine, New York, NY 10065; [c]Department of Radiology, Washington University School of Medicine in St. Louis, St. Louis, MO 63110; [d]Department of Pharmacology, Weill Cornell Medicine, New York, NY 10021; and [e]Molecular Pharmacology Program, Sloan Kettering Institute, Memorial Sloan Kettering Cancer Center, New York, NY 10065

1. E. Morgan *et al.*, The current and future incidence and mortality of gastric cancer in 185 countries, 2020–40: A population-based modelling study. *EClinicalMedicine* **47**, 101404 (2022).
2. F. Grillo, M. Fassan, F. Sarocchi, R. Fiocca, L. Mastracci, HER2 heterogeneity in gastric/gastroesophageal cancers: From benchside to practice. *World J. Gastroenterol.* **22**, 5879–5887 (2016).
3. S. Watson *et al.*, Combined HER2 analysis of biopsies and surgical specimens to optimize detection of trastuzumab-eligible patients in eso-gastric adenocarcinoma: A GERCOR study. *Ann. Oncol.* **24**, 3035–3039 (2013).
4. Y. C. Chung, J. F. Kuo, W. C. Wei, K. J. Chang, W. T. Chao, Caveolin-1 dependent endocytosis enhances the chemosensitivity of HER-2 positive breast cancer cells to trastuzumab emtansine (T-DM1). *PLoS One* **10**, e0133072 (2015).
5. D. Gajria, S. Chandarlapaty, HER2-amplified breast cancer: Mechanisms of trastuzumab resistance and novel targeted therapies. *Expert Rev. Anticancer Ther.* **11**, 263–275 (2011).
6. K. S. Gunturu, Y. Woo, N. Beaubier, H. E. Remotti, M. W. Saif, Gastric cancer and trastuzumab: First biologic therapy in gastric cancer. *Ther. Adv. Med. Oncol.* **5**, 143–151 (2013).
7. A. F. Okines, D. Cunningham, Trastuzumab: A novel standard option for patients with HER-2-positive advanced gastric or gastro-oesophageal junction cancer. *Therap. Adv. Gastroenterol.* **5**, 301–318 (2012).
8. J. Shi *et al.*, The HER4-YAP1 axis promotes trastuzumab resistance in HER2-positive gastric cancer by inducing epithelial and mesenchymal transition. *Oncogene* **37**, 3022–3038 (2018).
9. Z. Yang *et al.*, Acquisition of resistance to trastuzumab in gastric cancer cells is associated with activation of IL-6/STAT3/Jagged-1/Notch positive feedback loop. *Oncotarget* **6**, 5072–5087 (2015).
10. Q. Zuo *et al.*, Development of trastuzumab-resistant human gastric carcinoma cell lines and mechanisms of drug resistance. *Sci. Rep.* **5**, 11634 (2015).
11. H. Li *et al.*, MMP7 induces T-DM1 resistance and leads to the poor prognosis of gastric adenocarcinoma via a DKK1-dependent manner. *Anticancer Agents Med. Chem.* **18**, 2010–2016 (2018).
12. P. C. Thuss-Patience *et al.*, Trastuzumab emtansine versus taxane use for previously treated HER2-positive locally advanced or metastatic gastric or gastro-oesophageal junction adenocarcinoma (GATSBY): An international randomised, open-label, adaptive, phase 2/3 study. *Lancet Oncol.* **18**, 640–653 (2017).
13. K. Shitara *et al.*, Trastuzumab deruxtecan in previously treated HER2-positive gastric cancer. *N. Engl. J. Med.* **382**, 2419–2430 (2020).
14. F. Bensch *et al.*, (89)Zr-trastuzumab PET supports clinical decision making in breast cancer patients, when HER2 status cannot be determined by standard work up. *Eur. J. Nucl. Med. Mol. Imaging* **45**, 2300–2306 (2018).
15. P. Bhusari *et al.*, Development of Lu-177-trastuzumab for radioimmunotherapy of HER2 expressing breast cancer and its feasibility assessment in breast cancer patients. *Int. J. Cancer* **140**, 938–947 (2017).
16. G. L. Ray *et al.*, Pre-clinical assessment of Lu-labeled trastuzumab targeting HER2 for treatment and management of cancer patients with disseminated intraperitoneal disease. *Pharmaceuticals (Basel)* **5**, 1–15 (2011).
17. G. A. Ulaner, D. M. Hyman, S. K. Lyashchenko, J. S. Lewis, J. A. Carrasquillo, 89Zr-trastuzumab PET/CT for detection of human epidermal growth factor receptor 2-positive metastases in patients with human epidermal growth factor receptor 2-negative primary breast cancer. *Clin. Nucl. Med.* **42**, 912–917 (2017).
18. G. A. Ulaner *et al.*, Detection of HER2-positive metastases in patients with HER2-negative primary breast cancer using 89Zr-trastuzumab PET/CT. *J. Nucl. Med.* **57**, 1523–1528 (2016).
19. M. Kameswaran, U. Pandey, N. Gamre, H. D. Sarma, A. Dash, Preparation of (177)Lu-trastuzumab injection for treatment of breast cancer. *Appl. Radiat. Isot.* **148**, 184–190 (2019).
20. E. Hindie, P. Zanotti-Fregonara, M. A. Quinto, C. Morgat, C. Champion, Dose deposits from 90Y, 177Lu, 111In, and 161Tb in micrometastases of various sizes: Implications for radiopharmaceutical therapy. *J. Nucl. Med.* **57**, 759–764 (2016).
21. K. Kim, S. J. Kim, Lu-177-based peptide receptor radionuclide therapy for advanced neuroendocrine tumors. *Nucl. Med. Mol. Imaging* **52**, 208–215 (2018).
22. L. O. Dierickx, B. Severine, M. Fatima, B. Amel, G. Rosine, Successful and safe treatment with 177Lu-DOTATATE (Lutathera) of progressive metastatic pancreatic neuroendocrine tumor under hemodialysis. *Clin. Nucl. Med.* **45**, e400–e402 (2020).
23. M. Hamiditabar *et al.*, Safety and effectiveness of 177Lu-DOTATATE peptide receptor radionuclide therapy after regional hepatic embolization in patients with somatostatin-expressing neuroendocrine tumors. *Clin. Nucl. Med.* **42**, 822–828 (2017).
24. A. Mejia *et al.*, Peptide receptor radionuclide therapy implementation and results in a predominantly gastrointestinal neuroendocrine tumor population: A two-year experience in a nonuniversity setting. *Medicine (Baltimore)* **101**, e28970 (2022).
25. O. Sartor *et al.*, Lutetium-177-PSMA-617 for metastatic castration-resistant prostate cancer. *N. Engl. J. Med.* **385**, 1091–1103 (2021).
26. P. M. R. Pereira *et al.*, Caveolin-1 mediates cellular distribution of HER2 and affects trastuzumab binding and therapeutic efficacy. *Nat. Commun.* **9**, 5137 (2018).
27. A. Sorkin, L. K. Goh, Endocytosis and intracellular trafficking of ErbBs. *Exp. Cell Res.* **314**, 3093–3106 (2008).
28. C. Yang *et al.*, The role of caveolin-1 in the biofate and efficacy of anti-tumor drugs and their nano-drug delivery systems. *Acta Pharm. Sin. B* **11**, 961–977 (2021).
29. S. S. Park, J. E. Kim, Y. A. Kim, Y. C. Kim, S. W. Kim, Caveolin-1 is down-regulated and inversely correlated with HER2 and EGFR expression status in invasive ductal carcinoma of the breast. *Histopathology* **47**, 625–630 (2005).
30. P. M. R. Pereira *et al.*, Temporal modulation of HER2 membrane availability increases pertuzumab uptake and pretargeted molecular imaging of gastric tumors. *J. Nucl. Med.* **60**, 1569–1578 (2019).
31. P. M. R. Pereira, K. Mandleywala, A. Ragupathi, J. S. Lewis, Acute statin treatment improves antibody accumulation in EGFR- and PSMA-expressing tumors. *Clin. Cancer Res.* **26**, 6215–6229 (2020).
32. P. M. R. Pereira *et al.*, Caveolin-1 temporal modulation enhances antibody drug efficacy in heterogeneous gastric cancer. *Nat. Commun.* **13**, 2526 (2022).
33. K. Hindler, C. S. Cleeland, E. Rivera, C. D. Collard, The role of statins in cancer therapy. *Oncologist* **11**, 306–315 (2006).
34. B. Emami *et al.*, Tolerance of normal tissue to therapeutic irradiation. *Int. J. Radiat. Oncol. Biol. Phys.* **21**, 109–122 (1991).
35. S. M. Larson, J. A. Carrasquillo, N. K. Cheung, O. W. Press, Radioimmunotherapy of human tumours. *Nat. Rev. Cancer* **15**, 347–360 (2015).
36. T. Nubel, J. Damrot, W. P. Roos, B. Kaina, G. Fritz, Lovastatin protects human endothelial cells from killing by ionizing radiation without impairing induction and repair of DNA double-strand breaks. *Clin. Cancer Res.* **12**, 933–939 (2006).
37. V. Ziegler *et al.*, Rho inhibition by lovastatin affects apoptosis and DSB repair of primary human lung cells in vitro and lung tissue in vivo following fractionated irradiation. *Cell Death Dis.* **8**, e2978 (2017).
38. Y. Y. Janjigian *et al.*, First-line pembrolizumab and trastuzumab in HER2-positive oesophageal, gastric, or gastro-oesophageal junction cancer: An open-label, single-arm, phase 2 trial. *Lancet Oncol.* **21**, 821–831 (2020).
39. S. Mitani, H. Kawakami, Emerging targeted therapies for HER2 positive gastric cancer that can overcome trastuzumab resistance. *Cancers (Basel)* **12**, 400 (2020).
40. E. Obrador *et al.*, Radioprotection and radiomitigation: From the bench to clinical practice. *Biomedicines* **8**, 461 (2020).
41. G. Fritz, C. Henninger, J. Huelsenbeck, Potential use of HMG-CoA reductase inhibitors (statins) as radioprotective agents. *Br. Med. Bull.* **97**, 17–26 (2011).
42. X. Zhao *et al.*, Simvastatin attenuates radiation-induced tissue damage in mice. *J. Radiat. Res.* **55**, 257–264 (2014).
43. W. E. Bolch, K. F. Eckerman, G. Sgouros, S. R. Thomas, MIRD pamphlet No. 21: A generalized schema for radiopharmaceutical dosimetry–standardization of nomenclature. *J. Nucl. Med.* **50**, 477–484 (2009).
44. L. M. Carter *et al.*, PARaDIM: A PHITS-based monte carlo tool for internal dosimetry with tetrahedral mesh computational phantoms. *J. Nucl. Med.* **60**, 1802–1811 (2019).
45. T. Sato *et al.*, Overview of particle and heavy ion transport code system PHITS. *Ann. Nucl. Energy* **82**, 110–115 (2015).